J.Natn.Sci.Foundation Sri Lanka 2025 53 (3): 293 - 306
DOI: http://dx.doi.org/10.4038/jnsfsr.v53i3.12590

RESEARCH ARTICLE

Agricultural Engineering

Effect of temperature on drying kinetics and quality attributes of coffee beans during hot air drying

AJ Fernando[*1,2] , KSP Amaratunga[3], DAN Dharmasena[3], and THKR De Silva[4]
[1] *Department of Agricultural Engineering and Soil Science, Faculty of Agriculture, Rajarata University of Sri Lanka, Anuradhapura, Sri Lanka.*
[2] *Postgraduate Institute of Agriculture, University of Peradeniya, Peradeniya, Sri Lanka.*
[3] *Department of Agricultural Engineering, Faculty of Agriculture, University of Peradeniya, Peradeniya, Sri Lanka.*
[4] *Department of Mathematics, Faculty of Science, University of Peradeniya, Peradeniya, Sri Lanka.*

Submitted: 09 March 2025; Revised: 29 July 2025; Accepted: 28 August 2025

Abstract: This study systematically investigates the thin-layer drying kinetics of coffee (*Coffea arabica*) cherries during hot air drying, with experiments conducted at four distinct temperatures: 40 °C, 60 °C, 80 °C, and 100 °C. A comprehensive analysis was performed using ten widely recognized mathematical models: Newton, Page, Modified Page, Henderson and Pabis, Logarithmic, Two-Term, Exponential Two-Term, Diffusion Approximation, Midilli, and Singh to model the experimental moisture ratio data and characterize drying behavior. The drying process was characterized by a predominant falling rate period, indicating that internal moisture diffusion governs the kinetics. Among the models evaluated, the Midilli model best fits the experimental data, achieving the highest R^2 (0.9952 at 40 °C, 0.9973 at 60 °C, 0.9994 at 80 °C, and 0.9995 at 100 °C) and the lowest *RMSE* values (0.0793% at 40 °C, 0.2092% at 60 °C, 0.0624% at 80 °C, and 0.0868% at 100 °C). Furthermore, the effective moisture diffusivity increased significantly with temperature, ranging from 1.154×10^{-7} m²s^{-1} at 40 °C to 8.939×10^{-7} m²s^{-1} at 100 °C. The corresponding activation energy for the drying process was calculated as 32.36 kJ mol^{-1}. The L^* value (lightness) decreased consistently as the temperature increased. The findings of this study advance the understanding of coffee cherry drying kinetics under hot air conditions and offer practical insights for optimizing drying parameters. This research contributes a robust framework for designing and controlling industrial drying processes, ultimately enhancing product quality and energy efficiency in coffee production. The implications of these results are significant for scaling up operations and reducing energy consumption in drying systems.

Keywords: Coffee, drying, midilli model, moisture diffusivity, thin layer drying.

INTRODUCTION

Coffee is one of the world's most cherished beverages, celebrated for its unique aroma and rich flavour. In 2024, the global coffee market was valued at USD 97.71 billion, with projections indicating growth to USD 102.98 billion by 2025 and reaching USD 156.85 billion by 2033, a compound annual growth rate of 5.4% from 2025 to 2033 (Straits Research, 2025). Various products fuel this expansive market, including roasted, instant, and ready-to-drink coffees. Recent analyses show robust global consumption, with European consumers accounting for a significant market share (International Coffee Organization [ICO], 2022). The beverage's popularity largely stems from its unique organoleptic properties, which are closely tied to postharvest processing techniques. Processes such as cherry harvesting, de-pulping, fermentation, drying, and storage initiate complex chemical transformations in green coffee beans, ultimately shaping the quality of the final brew (Huch & Franz, 2015; Sunarharum *et al.*, 2014).

Following harvest, coffee cherries undergo primary processing through one of three main methods: natural

* Corresponding author (jayaruwanifernando@gmail.com; https://orcid.org/0000-0003-2292-547X)

drying, wet processing, or semi-dry processing (Elhalis *et al.*, 2023). The choice of method and its duration depend on factors such as available resources, climatic conditions, and the intended quality of the final product. The natural drying method involves non-selective harvesting, either by hand or with machinery, followed by spreading the cherries on drying surfaces or the ground under direct sunlight for approximately 20 to 30 days. During this period, moisture content gradually reduces from 60-65% wet basis (wb) to around 12% (Silva *et al.*, 2000). Mechanical dryers can be used independently or in combination with solar drying to accelerate the drying process. However, precise control of the drying process is necessary, as excessive or inadequate drying can lead to chemical changes in the beans, ultimately influencing the quality of the final coffee product (Do Carmo *et al.*, 2020).

Drying is a crucial preservation method that reduces the moisture content of agricultural products, thereby lowering shipping costs and storage space requirements. In the case of coffee cherries, various drying techniques have been adopted to optimize efficiency and product quality. While traditional sun drying remains widely used, recent studies have explored alternative methods of drying. For instance, Deeto *et al.* (2018) demonstrated the effectiveness of solar drying for coffee cherries, and convective drying has been thoroughly investigated by Burmester and Eggers (2010), Nilnont *et al.* (2012), and Muhidong *et al.* (2013). Firdissa *et al.* (2022) reported that coffee beans processed using the semi-washed method and dried under natural sunlight and solar tunnel conditions achieved a specialty coffee Grade of Q1. Innovative approaches such as heat pump drying (Fernando *et al.*, 2021) and microwave drying (Ghosh & Venkatachalapathy, 2014) have emerged, offering promising alternatives to conventional techniques. These novel methods have the potential to enhance drying efficiency, improve product quality, and reduce energy consumption, making them valuable for modern coffee processing applications.

According to the American Society of Agricultural and Biological Engineers (ASABE) (2022), a thin layer is a uniformly thick layer of material exposed to air during drying, typically comprising no more than three layers of individual particles. This configuration facilitates the analysis of simultaneous heat and mass transfer processes during drying. Thin-layer drying has recently been studied by Salehi *et al.* (2024) for eggplant and Wang *et al.* (2024) for pelleted feed. While Phitakwinai *et al.* (2019) examined the thin-layer drying behavior of parchment coffee, the drying characteristics of coffee cherries under similar conditions remain unexplored. Consequently, this study aims to quantify the moisture transfer rate of coffee cherries across various temperature ranges using thin-layer drying data applicable to both drying and roasting processes. A best-fit mathematical model was utilized to develop a relationship for the drying coefficients of coffee cherries, and further analyses estimated the moisture diffusivity and activation energy of fresh coffee cherries. The findings from this research are expected to inform the design of a hot-air dryer for coffee cherries and provide recommendations for optimal drying conditions and process control.

MATERIALS AND METHODS

Coffee cherries

Freshly harvested *Coffea arabica* cherries were collected from plantations in Kandy, Sri Lanka (7.2906° N, 80.6337° E; approximately 500 m above sea level). The coffee cherries were visually examined to confirm uniform ripeness and manually cleaned to remove foreign material and defective fruits before conducting hot-air drying experiments.

Drying procedure

Drying experiments were carried out using a gravity convection laboratory oven (Fisher Scientific Econotemp Model 55G, USA). A thin layer (single layer) of coffee cherries was dried at four controlled temperatures: 40 °C, 60 °C, 80 °C, and 100 °C. The oven was preheated for one hour before each run to ensure thermal stability and steady-state conditions. While the oven provided precise temperature control, it lacked active airflow and humidity regulation. As a result, internal air velocity and relative humidity were not measured and may have fluctuated during the drying process. Nevertheless, gravity convection ovens are commonly used in thin-layer drying studies where temperature is the dominant parameter, and the setup provides sufficiently stable thermal conditions for modeling drying kinetics.

Moisture content was determined according to ISO Standard 11520-2 (International Standards Organization [ISO], 2001). Random samples of 10-15 g were collected, and each drying experiment was conducted in triplicate. The average moisture content was recorded for each sample and used in subsequent data analysis. The wet basis moisture content (MC_{wb}) of the coffee cherries was calculated using Equation 1.

$$MC_{wb} = \frac{Weight_{initial} - Weight_{final}}{Weight_{initial}} \times 100 \quad ...(1)$$

where Wi is the initial mass of the sample and Wd is the oven-dry mass of the sample.

Mathematical modeling

Estimation of effective moisture diffusivity

Liquid and vapor diffusion predominantly govern the falling-rate drying stage in agricultural produce. This moisture transport is modeled using Fick's second law of diffusion (Equation 2), where the effective diffusivity quantifies the rate of moisture movement (Hui *et al.*, 2008).

$$\frac{\partial MC}{\partial t} = \nabla^2 \times D_{eff} \times MC \quad \text{(Crank, 1975)} \qquad ...(2)$$

Doymaz (2012) noted that the effective moisture diffusion coefficient (D_{eff}) reflects a material's drying capacity under various conditions. Equation 3 presents a simplified form of Fick's second law of diffusion, assuming an initially uniform moisture distribution and an infinite slab geometry.

$$\mathrm{MR} = \frac{\mathrm{MC(t)} - \mathrm{MC(eq)}}{\mathrm{MC_0} - \mathrm{MC(eq)}} = \frac{8}{\pi^2}\sum_{n=0}^{\infty}\frac{1}{(2n+1)^2} \times exp\left[-(2n+1)^2 \ \frac{\pi^2 D_{eff}\ t}{L^2}\right] \qquad ...(3)$$

where $\mathrm{MC(t)}$ is the dry basis moisture content during the drying process, $\mathrm{MC_0}$ is the dry basis moisture content of a product before starting the drying process, $\mathrm{MC(eq)}$ is the equilibrium dry basis moisture content, and L is the slab thickness (m) (ASABE, 2022).

Equation 4 has been applied to coffee cherries, considering sphere geometry.

$$\mathrm{MR} = \frac{\mathrm{MC(t)} - \mathrm{MC(eq)}}{\mathrm{MC_0} - \mathrm{MC(eq)}} = \frac{6}{\pi^2}\sum_{n=0}^{\infty}\frac{1}{n^2}\ exp\left[-n^2 \ \frac{\pi^2 D_{eff}\ t}{r_s^2}\right] \qquad ...(4)$$

where r_s is the sphere radius (m) (Hui *et al.*, 2008). The assumptions for applying Equation 4 for coffee cherries were as follows: the diffusion coefficient is not dependent on the moisture content of a product at a given temperature, during the drying process the coffee cherries are isothermal, there is a uniform initial moisture content distribution in the initial stage of the coffee cherries, the coffee cherries surface moisture content rapidly reaches equilibrium with the surrounding air properties, and the coffee cherry size and geometry is not changing during the drying. Furthermore, there is no mass reduction or gain inside the coffee cherry (adapted from: Kahveci & Cihan, 2008).

Table 1: Thin-layer drying models and their applications

Thin-layer drying models	**Applications**
Semi-theoretical models	
Models derived from Newton's law of cooling	
Lewis model / Newton/Simple/Exponential model $\mathrm{MR} = \frac{\mathrm{MC(t)} - \mathrm{MC(eq)}}{\mathrm{MC_0} - \mathrm{MC(eq)}} = \exp(-\mathrm{k_0 t})$ Lewis (1921)	Red chili (Hossain *et al.*, 2007), Soyabeans (Coradi *et al.*, 2022), Maize (Mondal *et al.*, 2022)
Page model $\mathrm{MR} = \frac{\mathrm{MC(t)} - \mathrm{MC(eq)}}{\mathrm{MC_0} - \mathrm{MC(eq)}} = \exp(-\mathrm{k_0 t^n})$ Page (1949)	Mint leaves (Ramirez-Gutierrez *et al.*, 2021), White mushrooms (Szadzińska & Mierzwa, 2021), Pomegranate (Adetoro *et al.*, 2020)
Modified Page model $\mathrm{MR} = \frac{\mathrm{MC(t)} - \mathrm{MC(eq)}}{\mathrm{MC_0} - \mathrm{MC(eq)}} = \exp[(-\mathrm{k_0 t})^n]$ White *et al.* (1980)	Pumpkin (Semai *et al.*, 2021), Red kidney beans (Jian & Jayas, 2018)

Thin-layer drying models	Applications
Models derived from Fick's second law of diffusion	
Henderson and Pabis model $MR = \frac{MC(t) - MC(eq)}{MC_0 - MC(eq)} = a \exp(-k_0 t)$ Henderson & Pabis, 1961	Paddy (Golpour *et al.*, 2021), Dill leaves (Dikmen *et al.*, 2019)
Logarithmic model $MR = \frac{MC(t) - MC(eq)}{MC_0 - MC(eq)} = a \times \exp(-k_0 t) + C$ Chandra & Singh, 1995	Sweet basil (Dikmen *et al.*, 2019), Yam (Kamal *et al.*, 2020)
Two-term model $MR = \frac{MC(t) - MC(eq)}{MC_0 - MC(eq)} = a \exp(-k_0 t) + b \exp(-k_1 t)$ Henderson, 1974	Rough rice (Foroughi-Dahr *et al.*, 2015), Parsley (Dikmen *et al.*, 2019)
Exponential two-term model $MR = \frac{MC(t) - MC(eq)}{MC_0 - MC(eq)} = a \exp(-k_0 t) + (1 - a) \exp(-k_0 a t)$ Sharaf-Eldeen *et al.*, 1980	Starfruit slices (Dash *et al.*, 2013), Radish (Lee & Kim, 2009)
Approximation of diffusion $MR = \frac{MC(t) - MC(eq)}{MC_0 - MC(eq)} = a \exp(-k_0 t) + (1 - a) \exp(-k_0 b t)$ Kaseem, 1998	Apricot (Zhang *et al.*, 2016), Yam slices (Sobukola *et al.*, 2008)
Midilli model $MR = \frac{MC(t) - MC(eq)}{MC_0 - MC(eq)} = a \exp(-k_0 t^n) + bt$ Midilli *et al.*, 2002	Pomegranate (Adetoro *et al.*, 2020), Mango (Mugodo & Workneh, 2021)
Empirical models	
Wang and Singh model $MR = 1 + bt + at^2$ Chen & Wu, 2001	Banana (Kadam & Dhingra, 2011; Omolola *et al.*, 2014;), Nata de coco (Fan *et al.*, 2011)

MR: moisture ratio, MC(t): moisture content at time t (dry basis), MC: initial moisture content (dry basis), MC(eq): equilibrium moisture content (dry basis), a, b, C, n: model constants, k_0, k_1: drying rate constants, t: time

Thin-layer drying models

The drying kinetics of most agricultural products predominantly occur during the falling-rate period and are typically predicted using theoretical, semi-theoretical, and empirical models. Table 1 lists ten widely used thin-layer drying models for determining the moisture ratio in various agricultural materials.

Activation energy

Arrhenius' equation describes the effect of drying temperature on the effective moisture diffusion coefficient (Equation 5) (Kashaninejad *et al.*, 2007; Perea-Flores *et al.*, 2012).

$$D_{eff} = D_0 \exp\left(-\frac{E_a}{RT}\right) \quad ...(5)$$

where D_0 is the diffusivity constant at infinite temperature, E_a is the activation energy (kJ mol^{-1}), R is the universal gas constant (8.314 J mol^{-1} K^{-1}), and T is the drying temperature in K.

Model parameter estimation and data analysis

Model fitting was conducted using a non-linear optimization method in Excel Solver, utilizing the generalized reduced gradient (GRG) non-linear algorithm. This method was employed to estimate the model parameters by minimizing the sum of squared errors between the experimental and predicted moisture ratio (MR) values. The obtained model parameters were specific to each drying condition, and different models were compared to select the best-fit equation that accurately describes the drying kinetics.

To evaluate the quality and validity of the fitted models, the coefficient of determination (R^2) and root mean square error (*RMSE*) were calculated. The R^2 quantifies the model's ability to predict future outcomes by assessing the agreement between measured and predicted values (Hossain *et al.*, 2007). R^2 values range from 0 to 1, with values closer to 1 indicating a stronger correlation between experimental data and model predictions (Neter *et al.*, 1990). The R^2 is indicated by Equation 6.

$$R^2 = 1 - \frac{Residual\ sums\ of\ square}{Corrected\ total\ sums\ of\ square} \quad ...(6)$$

The differences between the model-predicted value and the observed value are measured by *RMSE* (Equation 7). Therefore, *RMSE* is a good measure of accuracy, providing a single measure of predictive power that incorporates the residuals. However, *RMSE* should approach zero (Changrue *et al.*, 2008), indicating that the results are less deviated from the mathematical model.

$$RMSE = \left\{\frac{1}{N}\sum_{i=1}^{N}\left(MR_{exp,i} - MR_{pre,i}\right)^2\right\}^{\frac{1}{2}} \quad ...(7)$$

Colour difference (ΔE)

The colour values of the initial sample and final sample were measured to analyze the colour values (CIE - Commission Internationale de l'Eclairage L^*, a^*, and b^* values). The subscript '1' refers to the initial colour parameters of each sample at the beginning of the drying experiment. Subscript '2' refers to the colour at the time of measurement. Lightness-darkness (L^*), redness-greenness (a^*), and yellowness-blueness (b^*) are the corresponding colour coordinates.

Table 2: Colour scale

Colour change	Description
$\Delta E < 0.2$	No visible difference
$2 > \Delta E > 0.2$	Small difference
$3 > \Delta E > 2$	Colour difference visible with high quality screen
$6 > \Delta E > 3$	Colour difference visible with medium quality screen
$12 > \Delta E > 6$	High colour difference
$\Delta E > 12$	Different colours

Every colour measurement was performed in triplicate, and the average value was reported. The total colour difference (ΔE) was then determined using Equation 8, and the scale of ΔE is shown in Table 2 (Klement *et al.*, 2021).

$$\Delta E = \sqrt{(L_2^* - L_1^*)^2 + (a_2^* - a_1^*)^2 + (b_2^* - b_1^*)^2} \quad ...(8)$$

where subscript 1 and 2 refer to initial and final values.

Hue angle (h*)

Hue angle is one of the primary properties of a colour, as defined technically in the CIECAM02 model, and it is determined by Equation 9 (Suchta *et al.*, 2020). Hue angle, ranging from 0 to 360 degrees in the redness-greenness (a^*) and yellowness-blueness (b^*) planes, is based on the concept of equal perceived difference.

$$h^* = tan^{-1}\frac{b^*}{a^*}\ (°) \quad ...(9)$$

Colour saturation (C_{ab}^*)

The intensity of colour was measured by colour saturation (Schanda, 2007). Equation 10 was used to determine colour saturation.

$$C_{ab}^* = \sqrt{a^{*2} + b^{*2}} \quad ...(10)$$

Saturation (S_{ab})

The saturation (Schanda, 2007) of a colour is determined by a combination of light intensities, calculated using Equation 11. The most saturated colour is achieved by using a single wavelength at high intensity, such as laser light.

$$S_{ab} = \frac{C_{ab}^*}{\sqrt{C_{ab}^{*2} + L^{*2}}} \times 100\ (\%) \quad ...(11)$$

RESULTS AND DISCUSSION

Coffee cherries, initially containing approximately 70% moisture (wet basis), were dried until a constant moisture level was achieved. Figure 1 depicts the moisture content trajectories at drying temperatures of 40 °C, 60 °C, 80 °C, and 100 °C. The data demonstrate that moisture content declines continuously over time, with higher drying air temperatures markedly accelerating moisture removal and reducing total drying time. The drying curves did not exhibit a pre-heating phase or a constant rate period; the entire process occurred within the falling rate period. This observation indicates that moisture removal from the coffee cherries was predominantly governed by diffusion. These drying characteristics are consistent with those observed in other agricultural products, as reported for chili (Mihindukulasuriya & Jayasuriya, 2013; Fernando *et al.*, 2022), bay laurel leaves (Doymaz, 2014b), pomegranate (Adetoro *et al.*, 2020), apricot (Zhang *et al.*, 2016), and saffron petals (Sharayei *et al.*, 2018).

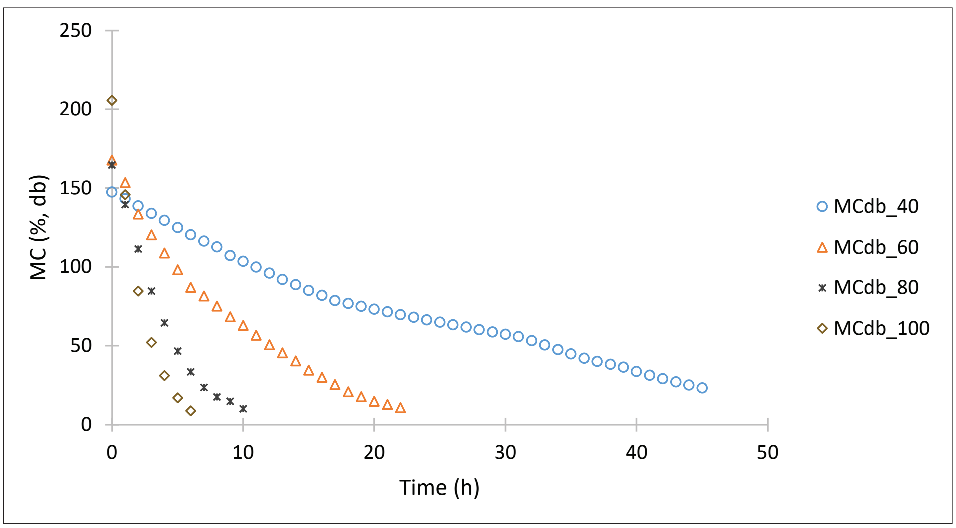

Figure 1: Moisture content variation of coffee cherries at different temperatures

The relationship between moisture content and drying time was evaluated by fitting the experimental data to various thin-layer drying models, as in Table 3. Further, Table 3 contains the constants for each model, along with the corresponding statistical analyses. All models exhibited high coefficients of determination (R^2 ranging from 0.9109 to 0.9998), confirming their suitability for characterizing the hot air drying behavior of coffee cherries.

Table 3: Model parameter values for the selected thin-layer drying models

Model	Model constants and coefficients	Drying Temperature			
		40°C	60°C	80°C	100°C
Newton (Lewis) $MR = \exp(-k_0 t)$	*k*	0.0361	0.1083	0.1622	0.4489
	R^2	0.9924	0.9955	0.9859	0.9960
	RMSE %	0.1410	0.1461	2.4305	0.1099
Page $MR = \exp(-k_0 t^n)$	*k*	0.0270	0.0885	0.0620	0.3657
	n	1.0862	1.0816	1.4848	1.2032
	R^2	0.9930	0.9957	0.9993	0.9995
	RMSE %	0.0877	0.5036	0.1753	0.0056

Model	Model constants and coefficients	Drying Temperature			
		40°C	60°C	80°C	100°C
Modified Page $MR = \exp[(-k_0 t)^n]$	*k*	0.0425	0.0736	0.0901	0.1498
	n	0.8500	1.4716	1.8011	2.9965
	R^2	0.9922	0.9955	0.9859	0.9960
	RMSE %	0.1310	0.0888	2.4041	0.1639
Henderson and Pabis $MR = a \exp(-k_0 t)$	*k*	0.0370	0.1100	0.1790	0.4608
	a	1.0224	1.0167	1.1183	1.0302
	R^2	0.9915	0.9949	0.9829	0.9958
	RMSE %	0.0863	0.2246	1.6413	0.1266
Logarithmic $MR = a \exp(-k_0 t) + C$	*k*	0.0291	0.0960	0.1564	0.4472
	a	1.1025	1.0392	1.1483	1.0369
	C	-0.1115	-0.0460	-0.0517	-0.0099
	R^2	0.9952	0.9976	0.9862	0.9960
	RMSE %	0.0891	0.2151	1.3225	0.3098
Two Term $MR = a \exp(-k_0 t) + b \exp(-k_1 t)$	k_0	0.0104	0.1100	0.1790	0.4608
	k_1	0.0256	0.1100	0.1790	0.4608
	a	-0.4070	0.3229	0.9676	0.9158
	b	1.3960	0.6939	0.1507	0.1144
	R^2	0.9951	0.9949	0.9829	0.9958
	RMSE %	0.0567	0.0183	1.0641	0.5094
Exponential Two Term $MR = a \exp(-k_0 t) + (1 - a) \exp(-k_0 a t)$	*k*	0.0444	3.9621	0.1622	0.4541
	a	1.5535	0.0265	0.9855	0.9090
	R^2	0.9934	0.9959	0.9859	0.9960
	RMSE %	0.0217	0.1103	2.4027	0.1404
Approximation of diffusion $MR = a \exp(-k_0 t) + (1 - a) \exp(-k_0 b t)$	*k*	0.0311	0.3426	0.1622	4.0247
	a	1.0539	-0.1210	0.1078	-0.2110
	b	-0.2205	0.3411	1.0000	0.1321
	R^2	0.9951	0.9956	0.9859	0.9998
	RMSE %	0.0247	0.3748	2.1030	0.1633
Midilli $MR = a \exp(-k_0 t^n) + bt$	*k*	0.0375	0.0951	0.0612	0.3675
	n	1.0060	1.0253	1.4989	1.2045
	a	-0.0015	0.9897	1.0021	1.0032
	b	0.9455	-0.0010	0.0003	0.0002
	R^2	0.9952	0.9973	0.9994	0.9995
	RMSE %	0.0793	0.2092	0.0624	0.0868
Wang and Singh $MR = 1 + bt + at^2$	*a*	-0.0285	-0.0729	-0.1096	-0.2205
	b	0.0002	0.0013	0.0029	0.0109
	R^2	0.9936	0.9883	0.9831	0.9109
	RMSE %	0.1070	1.2476	0.7832	4.5845

RMSE measures the average magnitude of the errors between the predicted and observed values. A lower *RMSE* indicates a closer fit to the data. At 40 °C and 60 °C, the Exponential Two-term model minimizes *RMSE*, meaning it has the lowest average error at these temperatures, even if its R^2 might not be the highest. At 80 °C and 100 °C, the Page model provides the lowest *RMSE* values, suggesting that although it may not explain the variability (R^2) as well as some other models, it offers the most accurate predictions regarding error magnitude.

Table 3 shows that the model that explains the most variability (high R^2) is not always the same as the one that minimizes error (low *RMSE*). This difference implies that the choice of model might depend on whether the priority is to understand the underlying process (explained variance) or to achieve precise predictions (minimal error). When choosing a model for practical applications, researchers might weigh whether they need one that best explains the data variability (using R^2) or one that offers the most precise predictions (using *RMSE*). Table 3 suggests that the optimal choice can shift with operating conditions, such as temperature, and that sometimes, a trade-off between explained variance and error minimization is necessary.

When evaluating the entire dataset, the Midilli model stands out with exceptionally high R^2 values at all temperatures: 0.9952 at 40 °C, 0.9973 at 60 °C, 0.9994 at 80 °C, and 0.9995 at 100 °C. These figures demonstrate that the model accounts for nearly all the variability in the drying data. Additionally, it maintains impressively low *RMSE* values, 0.0793% at 40 °C, 0.2092% at 60 °C, 0.0624% at 80 °C, and 0.0868% at 100 °C, indicating that its predictions closely match the observed values. The consistently high R^2 and low *RMSE* across all conditions confirm that the Midilli model explains the data's variability and makes highly accurate predictions.

Figure 2 presents the experimental moisture ratio profiles alongside the predictions from the Midilli model at various drying air temperatures over time. The close agreement between observed data and model predictions underscores the superior fit provided by the Midilli model in capturing the drying behavior of coffee cherries. This robust performance corroborates findings reported for other agricultural products, including mango (Mugodo & Workneh, 2021), pomegranate (Adetoro *et al.*, 2020), apricot (Zhang *et al.*, 2016), jackfruit (Saxena & Dash, 2015), bay laurel leaves (Doymaz, 2014b), turnip slices (Kaveh & Amiri Chayjan, 2017), peach (Doymaz, 2014a), apple slices (Zarein *et al.*, 2013), kiwifruit (Darıcı & Şen, 2015), chili (Mihindukulasuriya & Jayasuriya, 2013), and pepper (Darvishi *et al.*, 2014). These results highlight the model's effectiveness as a predictive tool for thin-layer drying kinetics. They reinforce its potential application in optimizing drying processes for coffee cherries and other agricultural materials.

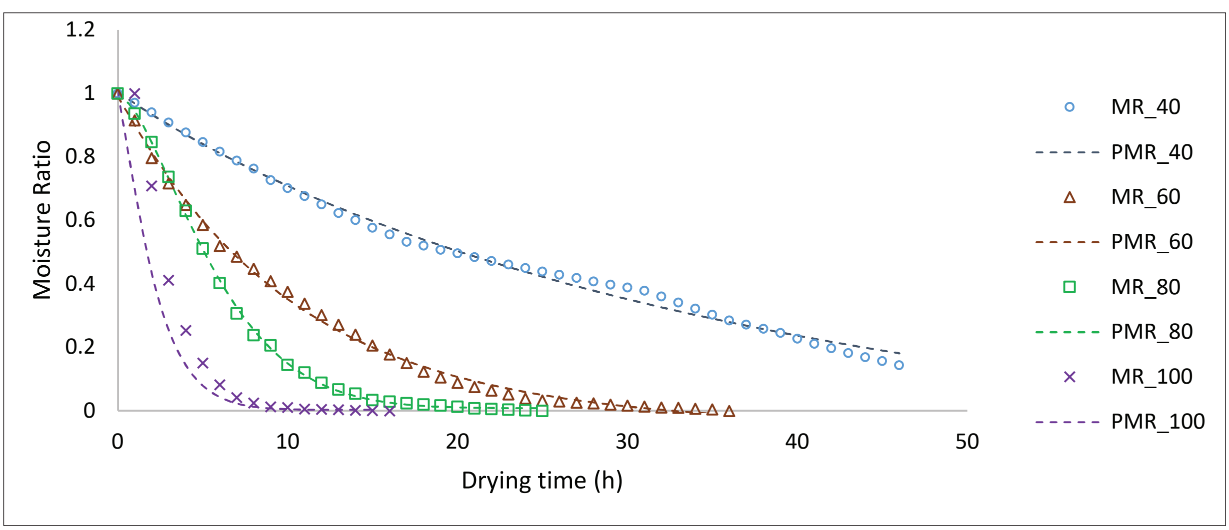

Figure 2: Experimental and predicted moisture ratios for coffee cherries applied to Midilli model

Table 4 presents the values of D_{eff} of coffee cherries at various temperatures. The effective moisture diffusivity was increased by increasing the drying air temperature from 40 °C to 100 °C.

Table 4: Effective diffusivity for coffee cherries at various temperatures

Temperature (°C)	Effective diffusivity (D_{eff}) (m^2s^{-1})
40	1.154×10^{-7}
60	3.276×10^{-7}
80	5.257×10^{-7}
100	8.939×10^{-7}

Diffusivity typically follows an Arrhenius relationship, meaning that as the temperature increases, the exponential increase in molecular movement leads to a higher effective diffusivity. In their study on the evolution and modeling of moisture diffusion in walnuts during combined hot air and microwave-vacuum drying, Man *et al.* (2024) found that the effective diffusivity (D_{eff}) increases with higher hot air temperatures. This increase is primarily due to the elevated temperature enhancing the kinetic energy of water molecules, thereby accelerating moisture diffusion (Lu *et al.*, 2020). Similarly, An *et al.* (2024) observed that when hot air temperature ranged from 30 to 45 °C, diffusivity varied between 2.190×10^{-9} and 3.022×10^{-9} m^2s^{-1} during the microwave hot air combined drying of peanut pods. Their findings indicate that a gradual increase in microwave power significantly impacts the moisture diffusion coefficient as the rising temperature augments the thermal energy within the water molecules of peanut pods, enhancing their mobility. Consequently, this increased energy transfer facilitates water molecules in overcoming their bonds, leading to more active moisture diffusion (Mohammadi *et al*., 2019).

Equation 5 was rearranged as in Equation 12 to determine the activation energy.

$$\ln(D_{eff}) = \ln(D_0) - \frac{E_a}{RT} \quad ...(12)$$

Values of D_{eff} were calculated using Equation 8 for the coffee cherry drying experiments, plotted in Figure 3. The plot demonstrates a straight line in the experimental drying air temperature range. The activation energy was calculated to be 32.358 kJ mol^{-1} from the slope of the straight line, as predicted by the Arrhenius equation.

Table 5 compares the activation energy

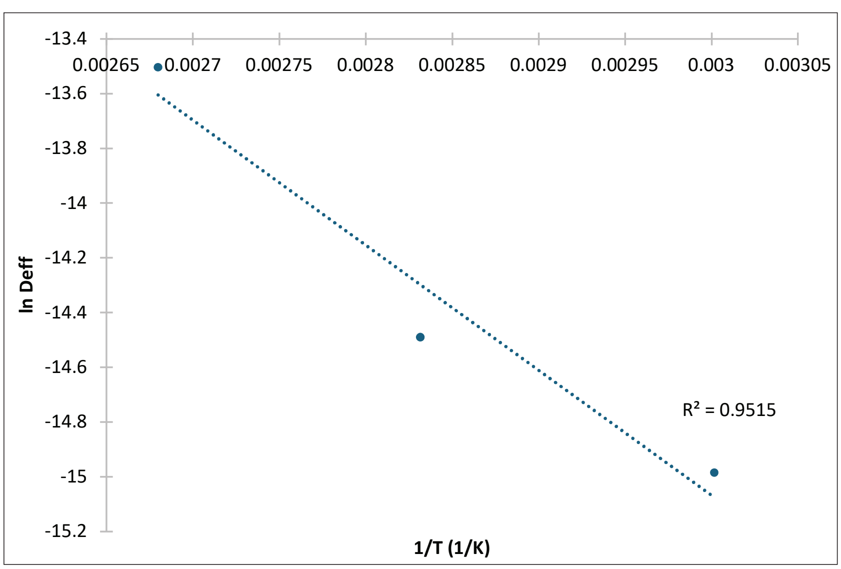

Figure 3: Logarithmic value of effective moisture diffusivity of coffee cherry as a function of the reciprocal of absolute drying air temperature

(E_a) of coffee cherries with that of other agricultural products. The observed variations in E_a among different products are attributed to inherent structural differences, particularly in the strength of water binding. Materials with strongly bound water require higher activation energy for moisture removal, indicating higher resistance to drying (Bezerra *et al*., 2015).

Table 5: Activation energy for different products

Product	Activation energy (kJ mol^{-1})	Reference
Soybean	13.88	Niamnuy *et al*., 2012
Sweet sorghum stalk	24.10	Shen *et al*., 2011
Presoaked soybean	31.40	Irigoyen & Giner, 2014
Coffee cherries	32.36	Current research
Castor oil seeds	41.41	Perea-Flores *et al*., 2012
Passion fruit peel	29.57–34.73	Bezerra *et al*., 2015

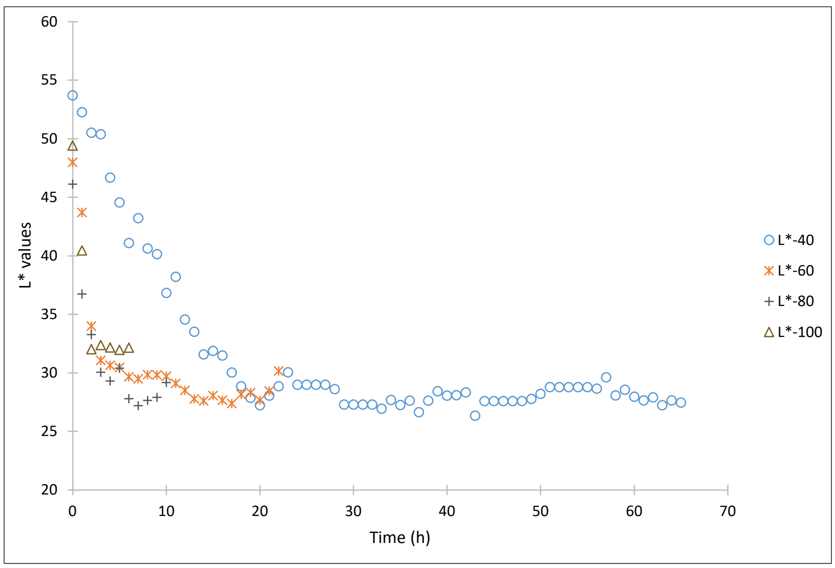

Figure 4: Lightness (L^*) values change during coffee drying at different temperatures

Table 6: Colour changes (ΔE) during coffee drying

Temperature (°C)	Colour coordinates	Before drying	After drying	Colour change (ΔE)
40	L^*	53.69 ± 1.6	27.94 ± 1.2	26.2
	a^*	-15.9 ± 0.3	5.48 ± 1.8	-19.7
	b^*	29.3 ± 2.4	5.73 ± 0.8	24.1
60	L^*	47.99 ± 2.0	27.27 ± 0.5	17.8
	a^*	-13.6 ± 5.2	5.49 ± 0.5	-18.9
	b^*	25.5 ± 1.1	5.79 ± 0.4	23.3
80	L^*	46.12 ± 2.5	27.4 ± 1.2	16.9
	a^*	1.07 ± 5.4	9.31 ± 1.6	-5.7
	b^*	23.99 ± 3.8	8.91 ± 1.4	16.6
100	L^*	49.41 ± 2.7	29.99 ± 0.5	17.3
	a^*	-10.6 ± 4.6	6.94 ± 0.5	-16.7
	b^*	22.66 ± 3.0	11.91 ± 0.2	14.2

The L^* value (lightness) drops at all drying temperatures. Drying removes water from the cherries, concentrating the natural pigments and increasing light absorption, which results in a darker appearance. Fresh coffee cherries exhibit negative a^* values, indicating a greenish colour. After drying, these values become positive, marking a shift toward red. The b^* value, which indicates yellowness, decreases markedly after drying.

Table 7: Colour properties of coffee during hot air drying

Temperature (°C)	Hue angle		Colour saturation		Saturation	
	Before drying	After drying	Before drying	After drying	Before drying	After drying
40	-1.07	0.81	33.34	7.93	52.75	0.27
60	-1.08	0.81	28.90	7.98	51.59	0.28
80	1.53	0.76	24.01	12.89	46.18	0.43
100	-1.13	1.04	25.02	13.78	45.17	0.42

Although the hue angle values are relatively small, the consistent shift from near-zero or slightly negative to positive values reinforces the observed change in a^* (from greenish to reddish). This shift indicates a subtle change in the overall tone of the cherries, consistent with pigment degradation and the formation of oxidation products. Both colour saturation and the measured saturation values drop steeply after drying. These reductions suggest that drying significantly diminishes the vividness and intensity of the cherries' colour, resulting in a more muted, less vibrant appearance.

The observed colour change is primarily due to the Maillard reaction and caramelization initiated by heat (Lee *et al.*, 2022). Extended exposure to high temperatures further degrades the colour, resulting in a more pronounced darkening of the material. The primary factors contributing to this deterioration include Maillard reactions, oxidation, and changes in the surface structure (Ray *et al.*, 2022).

CONCLUSION

The drying time for coffee cherries was reduced while the drying air temperature was increased from 40 °C to 100 °C. Therefore, the coffee cherry drying process primarily occurs during the falling rate period of the typical drying curve. The Midilli model provided the most accurate description of the drying kinetics, achieving the highest R^2 and the lowest *RMSE* values. The effective diffusivity values ranged from 1.154×10^{-7} to 8.939×10^{-7} m^2s^{-1} for the temperature range 40 °C to 100 °C for coffee cherries. This indicates an increase in effective moisture diffusivity at higher temperatures of the drying air. The activation energy of moisture diffusion was 32.36 kJ mol^{-1}. Drying leads to significant darkening of coffee cherries due to moisture loss, changes in pigment concentration, and non-enzymatic browning. These results provide data for controlling the drying conditions of coffee cherries.

Acknowledgement

The authors would like to acknowledge the support given by Mr. Tharindu Madushanka, Ms. Yashmi Jayaweera, Ms. Manuri Wimalaweera, and Chanaka Gunathunga during data collection.

REFERENCES

Do Carmo, K.B., do Carmo, J.C.B., Krause, M. R., & Peterle, G. (2020). Sensory and physiological quality of Arabic coffee under different fermentation times. *Bioscience Journal, 36*(2). 429 - 438. https://doi.org/10.14393/BJ-v36n2a2020-43255

Doymaz, İ. (2012). Sun drying of seedless and seeded grapes. *Journal of Food Science and Technology,* 49, 214-220. https://doi: 10.1007/s13197-011-0272-9

Doymaz, I. (2014a). Suitability of thin-layer drying models for infrared drying of peach slices. *Journal of Food Processing and Preservation, 38*(6), 2232-2239. https://doi.org/10.1111/jfpp.12277

Doymaz, İ. (2014b). Thin-Layer Drying of Bay Laurel Leaves (*Laurus nobilis* L.). *Journal of Food Processing and Preservation, 38*(1), 449-456. https://doi.org/10.1111/j.1745-4549.2012.00793.x

Elhalis, H., Cox, J., & Zhao, J. (2023). Coffee fermentation: Expedition from traditional to controlled process and perspectives for industrialization. *Applied Food Research, 3*(1), 100253. https://doi.org/10.1016/j.afres.2022.100253

Fan, H., Wu, Y., Hu, X., Wu, J. & Liao, X. (2011). Characteristics of thin-layer drying and rehydration of nata de coco. *International Journal of Food Science Technology, 46*(7), 1438-1444. https://doi.org/10.1111/j.1365-2621.2011.02642.x

Fernando, A. J., & Amaratunga, S. (2022). Application of far-infrared radiation for sun-dried chili pepper (*Capsicum annum* L.): drying characteristics and color during roasting. *Journal of the Science of Food and Agriculture*, *102*(9), 3781-3787. https://doi.org/10.1002/jsfa.11726

Fernando, A. J., Amaratunga, K. S. P., Madhushanka, H. T. N., & Jayaweera, H. R. Y. S. (2021). Drying performance of coffee in a batch-type heat pump dryer. *Transactions of the ASABE, 64*(4): 1237-1245. https://doi: 10.13031/trans.14268

Firdissa, E., Mohammed, A., Berecha, G., & Garedew, W. (2022). Coffee drying and processing method influence quality of arabica coffee varieties (*Coffea arabica* L.) at Gomma I and Limmu Kossa, Southwest Ethiopia. *Journal of Food Quality*, *2022*(1), 9184374. https://doi.org/10.1155/2022/9184374

Foroughi-Dahr, M., Golmohammadi, M., Pourjamshidian, R., Rajabi-Hamaneh, M., & Hashemi, S.J. (2015). On the characteristics of thin-layer drying models for intermittent drying of rough rice. *Chemical Engineering Communications, 202*(8), 1024-1035. https://doi.org/10.1080/00986445.2014.900049

Ghosh, P., & Venkatachalapathy, N. (2014). Thin layer drying of hot-air assisted microwave drying of parchment coffee. *International Journal of Latest Trends in Engineering and Technology, 4*(4), 121-133.

Golpour, I., Guiné, R. P., Poncet, S., Golpour, H., Chayjan, A. R., & Parian, A. J. (2021). Evaluating the heat and mass transfer effective coefficients during the convective drying process of paddy (*Oryza sativa* L.). *Journal of Food Process Engineering, 44*(9)e13771. https://doi.org/10.1111/jfpe.13771

Henderson, S. M., & Pabis, S. (1961). Grain drying theory I: Temperature effect on drying coefficient. *Agricultural and Food Sciences, Engineering,* 6: 169–174. https://api.semanticscholar.org/CorpusID:208841650

Henderson, S. M. (1974). Progress in developing the thin layer drying equation. *Transactions of the ASAE 17*(6), 1167-1168. https://doi: 10.13031/2013.37052

Hossain, M. A., Woods, J. L., & Bala, B. K. (2007). Single-layer drying characteristics and colour kinetics of red chilli. *International Journal of Food Science and Technology, 42*(11):1367–75. doi:10.1111/j.1365-2621.2006.01414.x

Huch, M., & Franz, C. M. A. P. (2015). Coffee: fermentation and microbiota. In *Advances in fermented foods and beverages* (501-513). Woodhead Publishing. https://doi.org/10.1016/B978-1-78242-015-6.00021-9

Hui, Y. H., Clary, C., Farid, M. M., Fasina, O. O., Noomhorm, A., & Welti-Chanes, J. (2008). *Food Drying*. Science and Technology. DEStech Pub. Inc., PA, USA.

International Coffee Organization [ICO] (2022). World coffee consumption. https://www.ico.org/trade_statistics.asp

Irigoyen, R. T., & Giner, S. A. (2014). Drying-toasting kinetics of presoaked soybean in a fluidized bed. Experimental study and mathematical modeling with analytical solutions. *Journal of Food Engineering,* 128, 31-39. https://doi.org/10.1016/j.jfoodeng.2013.12.00

International Standards Organization [ISO] (2018). ISO 1446:2001 (R2018). Green coffee - Determination of water content - Basic reference method. Geneva, Switzerland: International Standard Organization.

Jian, F., & Jayas, D. S. (2018). Characterization of isotherms and thin-layer drying of red kidney beans, Part I: Choosing appropriate empirical and semi-theoretical models. *Drying Technology, 36*(14), 1696-1706. https://doi.org/10.1080/07373937.2017.1422514

Kadam, D. M., & Dhingra, D. (2011). Mass transfer kinetics of banana slices during osmo-convective drying. *Journal of Food Process Engineering, 34*(2), 511-532. https://doi.org/10.1111/j.1745-4530.2009.00373.x

Kahveci, K., & Cihan, A. (2008). *Drying of Food Materials: Transport Phenomena.* Nova Science Publishers Inc.

Kamal, M. M., Ali, M. R., Shishir, M. R. I., & Mondal, S. C. (2020). Thin-layer drying kinetics of yam slices, physicochemical, and functional attributes of yam flour. *Journal of Food Process Engineering, 43*(8), e13448. https://doi.org/10.1111/jfpe.13448

Kaseem, A. S. (1998). Comparative studies on thin layer drying models for wheat. In *13th International Congress on Agricultural Engineering*, Vol. 6, February 2–6, Morocco.

Kashaninejad, M., Mortazavi, A., Safekordi, A., & Tabil, L. G. (2007). Thin-layer drying characteristics and modeling of pistachio nuts. *Journal of Food Engineering, 78*(1), 98-108. https://doi.org/10.1016/j.jfoodeng.2005.09.007

Kaveh, M., & Chayjan, A. R. (2017). Modeling thin-layer drying of turnip slices under a semi-industrial continuous band dryer. *Journal of Food Processing and Preservation, 41*(2), e12778. https://doi.org/10.1111/jfpp.12778

Klement, I., Vilkovský, P., Vilkovská, T., Orłowski, K. A., Barański, J., Chuchala, D., & Suchta, A. (2021). The influence of drying temperature on color change of hornbeam and maple wood used as surface and inner layers of wood composites. *Applied Sciences, 11*(22), 10673. https://doi.org/10.3390/app112210673

Lee, J. H., & Kim, H. J. (2009). Vacuum drying kinetics of Asian white radish (*Raphanus sativus* L.) slices. *LWT-Food Science and Technology, 42*(1), 180-186. https://doi.org/10.1016/j.lwt.2008.05.017

Lee, S. Y., Ferdinand, V., & Siow, L. F. (2022). Effect of drying methods on yield, physicochemical properties, and total polyphenol content of chamomile extract powder. *Frontiers in Pharmacology* 13, 1003209. https://doi.org/10.3389/fphar.2022.1003209

Lewis W. K. (1921). The rate of drying of solid materials. *IandEC-Symposium of Drying, 3*(5):42.

Lu, Y. J., Ren, G. Y., Duan, X., Zhang, L. D., Ling, Z. Z. (2020). Moisture migration properties and quality changes of fresh in-shell peanuts during hot air drying. *Food Science,* 41, 86–92. 10.7506/spkx1002-6630-20190311-134

Man, X., Li, L., Fan, X., Zhang, H., Lan, H., Tang, Y., & Zhang, Y. (2024). Evolution and Modelling of the Moisture Diffusion in Walnuts during the Combination of Hot Air and Microwave–Vacuum Drying. *Agriculture, 14*(2), 190. https://doi.org/10.3390/agriculture14020190

Midilli, A., Kucuk, H., & Yapar, Z. (2002). A new model for single-layer drying. *Drying Technology,* 20:1503–1513. https://doi.org/10.1081/DRT-120005864

Mihindukulasuriya, S.D.F., & Jayasuriya, H.P.W. (2013). Mathematical modeling of drying characteristics of chilli in hot air oven and fluidized bed dryers. *Agricultural Engineering International: CIGR Journal* 15(1):154–66.

Mohammadi, I., Tabatabaekoloor, R., & Motevali, A. (2019). Effect of air recirculation and heat pump on mass transfer and energy parameters in drying of kiwi fruit slices. *Energy,* 170, 149-158. https://doi.org/10.1016/j.energy.2018.12.099

Mondal, M. H. T., Akhtaruzzaman, M., & Sarker, M. S. H. (2022). Modeling of dehydration and color degradation kinetics of maize grain for mixed flow dryer. *Journal of Agriculture and Food Research,* 9, 100359. https://doi.org/10.1016/j.jafr.2022.100359

Mugodo, K., & Workneh, T. S. (2021). The kinetics of thin-layer drying and modelling for mango slices and the influence of differing hot-air drying methods on quality. *Heliyon,* p.e07182. https://doi.org/10.1016/j.heliyon.2021.e07182

Muhidong, J., Mursalim, & Rahman, A. (2013). The effect of airflow rate on single-layer drying characteristics of Arabica coffee. *International Food Research Journal, 20*(4): 1633-1637. https://api.semanticscholar.org/CorpusID:127661196

Neter, J., Wasserman, W., & Kutner, M. H. (1990). Applied linear statistical models. In: *Regression Analysis of Variance and Experimental Designs*. Richard D. Irwin Inc., USA.

Niamnuy, C., Nachaisin, M., Poomsa-ad, N., & Devahastin, S. (2012). Kinetic modelling of drying and conversion/degradation of isoflavones during infrared drying of soybean. *Food Chemistry, 133*(3), 946–952. https://doi:10.1016/j.foodchem.2012.02.010

Nilnont, W., Thepa, S., Janjai, S., Kasayapanand, N., Thamrongmas, C., & Bala, B. K. (2012). Finite element simulation of coffee (*Coffea arabica*) drying. *Food and Bioproduct Processing, 90*(2), 341–350. https://doi.org/10.1016/j.fbp.2011.06.007

Omolola, A. O., Jideani, A. I. O., & Kapila, P. F. (2014). Modeling microwave-drying kinetics and moisture diffusivity of Mabonde banana variety. *International Journal of Agricultural and Biological Engineering, 7*(6):107–13. https://doi:10.3965/j.ijabe.20140706.013

Page, G. E. (1949). Factors influencing the maximum rates of air drying shelled corn in thin layers. MS Thesis, Department of Mechanical Engineering, Purdue University, West Lafayette, IN.

Perea-Flores, M. J., Garibay-Febles, V., Chanona-Pérez, J. J., Calderón- Domínguez, G., Méndez-Méndez, J. V., Palacios-González, E., & Gutiérrez-López G. F. (2012). Mathematical modelling of castor oil seeds (*Ricinus communis*) drying kinetics in a fluidized bed at high temperatures. *Industrial Crops and Products* 38, 64–71. https://doi.org/10.1016/j.indcrop.2012.01.008

Phitakwinai, S., Thepa, S., & Nilnont, W. (2019). Thin-layer drying of parchment Arabica coffee by controlling temperature and relative humidity. *Food Science & Nutrition, 7*(9), 2921-2931. https://doi.org/10.1002/fsn3.1144

Ramirez-Gutierrez, D. M., Ileleji, K. E., & Deering, A. J. (2021). Evaluation of Novel Portable Passive and Cabinet Solar Dryers in Sun Drying of Mint Leaves under Indiana Weather Conditions. *Transactions of the ASABE, 64*(3), pp.1083-1094. https://doi: 10.13031/trans.14208

Ray, A., Mohanty, S., Jena, S., Sahoo, A., Acharya, L., Panda, P. C., *et al.* (2022). Drying methods affects physicochemical characteristics, essential oil yield, and volatile composition of turmeric (*Curcuma longa* L.). *Journal of Applied Research on Medicinal and Aromatic Plants,* 26, 100357. https://doi.org/10.1016/j.jarmap.2021.100357

Salehi, F., Goharpour, K., & Kamran, H. R. (2024). Effects of different pretreatment techniques on the color indexes, drying characteristics and rehydration ratio of eggplant slices. *Results in Engineering*, *21*, 101690. https://doi.org/10.1016/j.rineng.2023.101690

Saxena, J., & Dash, K. K. (2015). Drying kinetics and moisture diffusivity study of ripe jackfruit. *International Food Research Journal, 22*(1):414–20.

Schanda, J. (Ed.). (2007). *Colorimetry: Understanding the CIE system*. John Wiley & Sons.

Semai, H., Bouhdjar, A., & Amari, A. (2021). An improved protocol for natural convective drying of pumpkin. *Food and Feed Research, 48*(1), 29-39. https://doi: https://doi.org/10.5937/ffr0-31341

Sharaf-Eldeen, Y. I., Blaisdell, J. L., & Hamdy, M. Y. (1980). A model for ear corn drying. *Transactions of ASAE,* 23:1261–1265, 1271. https://doi: 10.13031/2013.34757

Sharayei, P., Hedayatizadeh, M., Chaji, H., & Einafshar, S. (2018). Studying the thin-layer drying kinetics and qualitative characteristics of dehydrated saffron petals. *Journal of Food Processing and Preservation, 42*(9), p.e13677. https://doi: 10.1111/jfpp.13677

Shen, F., Peng, L., Zhang, Y., Wu, J., Zhang, X., Yang, G., Peng, H., Qi, H., & Deng, S. (2011). Thin-layer drying kinetics and quality changes of sweet sorghum stalk for ethanol production as affected by drying temperature. *Industrial Crops and Products, 34*(3), 1588–1594. https://doi.org/10.1016/j.indcrop.2011.05.027

Silva, C. F., Schwan, R. F., Dias, Ë. S., & Wheals, A. E. (2000). Microbial diversity during maturation and natural processing of coffee cherries of *Coffea arabica* in Brazil. *International Journal of Food Microbiology, 60* (2–3), 251–260. https://doi.org/10.1016/S0168-1605(00)00315-9

Sobukola, O. P., Dairo, O. U., & Odunewu, A. V. (2008). Convective hot air drying of blanched yam slices. *International Journal of Food Science and Technology,* 43:1233–1238. https://doi.org/10.1111/j.1365-2621.2007.01597.x

Straits Research. (2025, February 12). *Coffee market size, share & trends analysis report by product type (whole bean coffee, ground coffee, instant coffee, coffee pods, capsules), by distribution channels (on-trade, off-trade), by nature (conventional, organic), by grade (Arabica, Robusta,* *specialty, others), by application (hot drinks, ready-to-drink coffee, flavored beverages, food & beverage flavors, nutraceuticals, pharmaceuticals, cosmetics, others) and by region (North America, Europe, APAC, Middle East and Africa, LATAM) forecasts, 2025–2033* (Report Code: SRFB2811DR). https://straitsresearch.com/report/coffee-market

Suchta, A., Barański J., Orłowski, K., & Chuchała, D. (2020). The effect of drying intensity on the color changes of pine wood (*Pinus Sylvestris* L.). *Trieskove a Beztrieskove Obrabanie Dreva 12*, 79-84.

Sunarharum, W. B., Williams, D. J., & Smyth, H. E. (2014). Complexity of coffee flavor: A compositional and sensory perspective. *Food Research International,* 62, 315-325. https://doi.org/10.1016/j.foodres.2014.02.030

Szadzińska, J., & Mierzwa, D. (2021). The influence of hybrid drying (microwave-convective) on drying kinetics and quality of white mushrooms. *Chemical Engineering and Processing-Process Intensification,* 167,108532. https://doi.org/10.1016/j.cep.2021.108532

Wang, W., Chen, J., Jin, N., Wang, H., Wang, L., & Wu, J. (2024). Thin-Layer Drying Model, Drying Rate, and Effective Water Diffusion Coefficient of Pelleted Feed. *International Journal of Chemical Engineering*, *2024*(1), 7092556. https://doi.org/10.1155/2024/7092556

White, G. M., Bridges, T. C., Loewer, O. J., & Ross, I. J. (1980). Seed coat damage in thin layer drying of soybeans. *Transactions of the ASAE, 23*(1), 224-0227. https://doi: 10.13031/2013.34559

Zarein, M., Samadi, S., & Barat, G. (2013). Kinetic drying and mathematical modeling of apple slices on dehydration process. *Journal of Food Processing and Technology, 4*(7):1–4. https://doi:10.4172/2157-7110.1000247

Zhang, Q. A., Song, Y., Wang, X., Zhao, W. Q., & Fan, X. H. (2016). Mathematical modeling of debittered apricot (*Prunus armeniaca* L.) kernels during thin-layer drying. *CyTA-Journal of Food, 14*(4), 509-517. https://doi.org/10.1080/19476337.2015.1136843